Radial Position Active Control of Double Stator Axial Gap Self-bearing Motor for Paediatric VAD

Masahiro Osa[a], Toru Masuzawa[a], Naoki Omori[a], Eisuke Tatsumi[b]

[a] Ibaraki University, 4-12-1, Hitachi, Japan, osa@mx.ibaraki.ac.jp
[b] National Cerebral and Cardiovascular Center, 5-7-1 Fujishirodai, Suita, Japan

***Abstract*—A novel axial gap double stator self-bearing motor which can control five-degrees of freedom (5-DOF) of rotor postures have been developed for paediatric ventricular assist device (VAD). The motor has a top stator, a bottom stator and a levitated rotor driven as a synchronous permanent magnet motor. The rotor is axially suspended between the stators which have an identical structure. A double stator mechanism enhances a higher torque production and realizes radial position active control. This paper proposes a concept of radial position active control and magnetic suspension ability of developed self-bearing motor. The rotor is successfully levitated and rotated up to 6400 rpm without any physical contact with 5-DOF active control in air. The radial oscillation amplitudes are actively suppressed with the proposed radial position control concept. The developed 5-DOF controlled self-bearing motor which is suitably miniature as an actuator for paediatric VAD indicates sufficient capability of the magnetic levitation and non-contact rotation.**

I. INTRODUCTION

Mechanical circulatory supports have been clinically applied to adult heart failure patients due to the high rate of heart disease and the shortage of donor hearts. The successful use of ventricular assist devices (VADs) in adult patients over the last decade has led to increased interest in this technology for paediatric patients [1]-[4]. However, the majority of VADs for paediatric heart disease have been applied to patients older than 10 years due to limitations of device size and structural functionalities. Thus, demands for paediatric VADs specifically designed for both infants and small children have been recently promoted widely. The paediatric VADs has to satisfy following design requirements: 1) high durability for long term support of patients, 2) minimal blood damage and no thrombosis formation in the pump cavity, 3) miniature device size in order to be fully implanted in a small peritoneal cavity from birth to more than two years of age, and 4) wide operational range from 2000 rpm to 5000 rpm in order to regulate the pump flow rate according to growth of paediatric patients. Due to significant advantages of eliminating mechanical wear components compared to traditional contact bearing systems, application of magnetically suspended motors in VADs have been main focus of the research [5]-[8]. Magnetically suspended rotary VADs offers advantages of contactless motor drive such as high speed rotation, no material wear, zero friction, less heat generation, better durability and better blood compatibility of the devices. However, the magnetic air-gap of magnetically suspended motors applied for rotary VADs is quite larger than in case of typical industrial magnetic bearing applications in order to avoid blood cell destruction due to the high share stress. These circumstances grossly reduce a magnetic suspension force and torque capacity. This reduction of magnetic suspension force and torque causes both a deterioration of magnetic suspension stability and a reduction of motor energy efficiency. In this study, a novel 5-degrees of freedom (DOF) controlled axial gap double stator self-bearing motor was proposed to overcome magnetic performance drawbacks due to the large air-gap length. The objectives of this paper were to demonstrate the radial position control capability and examine the feasibility of miniaturized 5-DOF controlled motor for paediatric VAD.

II. MATERIALS AND METHODS

A. Structure and control principle of 5-DOF controlled self-bearing motor

The proposed 5-DOF controlled self-bearing motor shown in Fig. 1 is a permanent magnet synchronous motor which has a top stator, a bottom stator and a levitated rotor. The levitated rotor is axially sandwiched by both stators that have an identical structure. A double stator mechanism enhances a rotating torque production and also realizes the proposed 5-DOF active control of levitated rotor postures. Two types of concentrated windings are independently wound on each stator tooth. An axial position (z) and rotating speed (ω_z) of the rotor are regulated by using a vector control algorithm which can generate axial suspension force and rotating torque with a single rotating magnetic field [9]-[12]. The axial position of levitated rotor is actively regulated by field strengthening and field weakening as shown in Fig. 2.

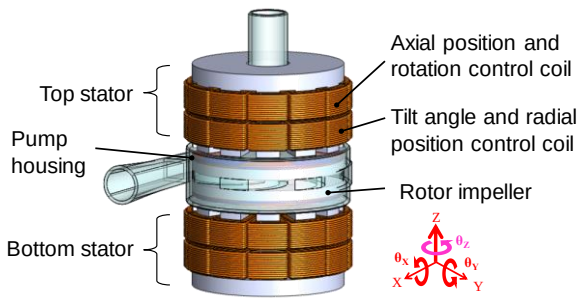

Figure 1. Schematic of proposed 5-DOF controlled axial gap double stator self-bearing motor for paediatric VAD

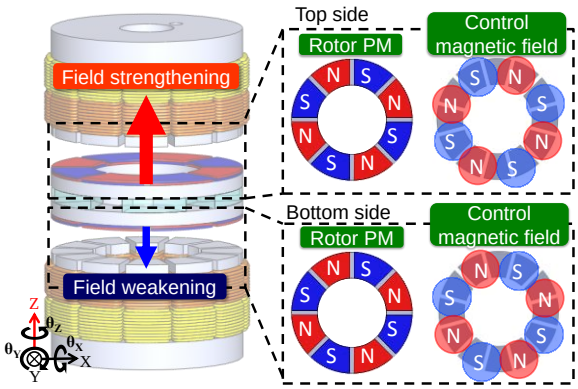

Figure 2. Principle of axial force production by utilizing field strengthning and field weakening

An axial attractive force F_z and a rotating torque $T_{\theta z}$ produced by the double stator are described by equation (1) and (2) using magnetic flux density produced by rotor permanent magnets B_p, inner and outer radius of rotor r_1 and r_2, pole pair number of rotor permanent magnet M, number of turns in windings N, air-gap length of z, d-axis current i_d and q-axis current i_q.

$$F_z = \sqrt{\frac{2}{3}} \frac{(r_2^2 - r_1^2)\pi B_p}{z} N i_d \qquad (1)$$

$$T_{\theta z} = \sqrt{\frac{2}{3}} (r_2^2 - r_1^2)\pi B_p N i_q \qquad (2)$$

From equation (1) and (2), axial attractive force and rotating torque are controlled independently with d-axis and q-axis current.

As shown in Fig. 3, a single rotating control flux density based on P±2 pole algorithm produces a restoring torque and a radial suspension force simultaneously [13]. The restoring torque and the radial suspension force can be produced independently with double stator mechanism. Fig. 4 shows the principles of inclination control around y-axis and radial position control in x direction of levitated rotor. Both stators produces restoring torque in the same direction; the radial forces produced by stators cancel each other, and the restoring torque produced as shown in Fig. 4(a). In contrast, the restoring torque produced by top stator and bottom stator is regulated in opposite direction, then the radial suspension force can be generated as shown in Fig. 4(b). In a similar manner, the inclination control around x-axis and the radial position control in y direction are available. Consequently, the inclination angles (θ_x, θ_y) and the radial positions (x, y) of levitated rotor can be controlled by regulating the magnitude and the direction of restoring torque and radial suspension force according to excitation currents fed into top stator and bottom stator.

When restoring torque and radial suspension force are proportional to excitation current, these are given by equation (3) and (4) using a restoring torque constant $k_{T\theta y}$ and a radial suspension force constant k_{Fx}.

$$T_{\theta y} = k_{T\theta y} i \qquad (3)$$

$$F_x = k_{Fx} i \qquad (4)$$

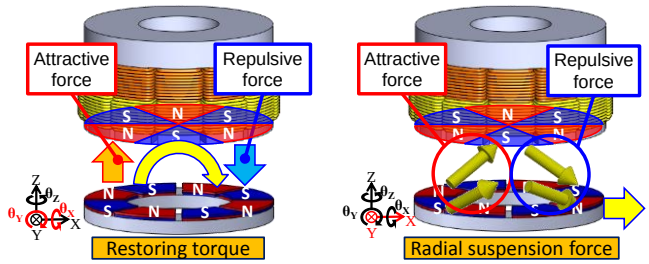

Figure 3. Principle of restoring torque and radial suspension force production by using single magnetic field based on P±2 pole algorithm

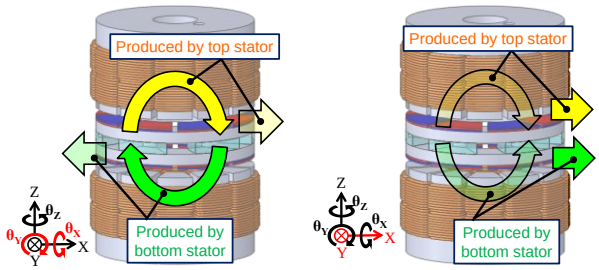

(a) (b)

Figure 4. Independently produced restoring torque and radial suspension force with double stator mechanism: (a) Restoring torque production, (b) Radial suspension force production

A total restoring torque and a radial suspension force acting on levitated rotor with double stator mechanism are given by equation (5) and (6) when excitation current of top stator and bottom stator are defined as i_{top} and i_{bottom} respectively.

$$T_{\theta y} = k_{T\theta y}(i_{top} + i_{bottom}) \qquad (5)$$

$$F_x = k_{Fx}(i_{top} - i_{bottom}) \qquad (6)$$

When the both excitation current i_{top} and i_{bottom} are equal, only the restoring torque can be produced. In that case, the motor is operated as 3-DOF controlled self-bearing motor.

The double stator mechanism with both vector control algorithm and P±2 pole algorithm offers 5-DOF control of the levitated rotor postures without any additional active or passive magnetic bearings. Thus, the proposed 5-DOF controlled self-bearing motor has advantages of compactness and simplification of device structure compare to conventional 5-DOF controlled maglev motors.

B. FEM analysis and fabrication of 5-DOF controlled self-bearing motor

The principle of radial suspension force production was confirmed by using three dimensional magnetic field FEM analysis. A pole pair combination and detailed geometries of proposed 5-DOF controlled self-bearing motor were determined in FEM analysis. A double stator axial gap self-bearing motor which has twelve motor stator slots and eight rotor poles shown in Fig. 5 were developed based on the results of FEM analysis. Fig. 6 shows the geometric parameters of developed motor stator and levitated rotor. The developed motor has an outer diameter of 28 mm, a height of 41 mm and a magnetic air-gap length of 1.5 mm. The weight of the levitated rotor is 25 g. The thickness of rotor permanent magnets are 0.7 mm. A core material of stator and rotor is

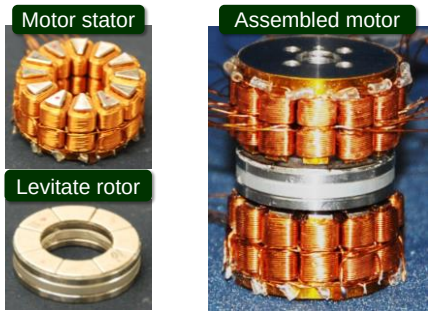

Figure 5. Photographs of developed 5-DOF controlled self-bearing motor

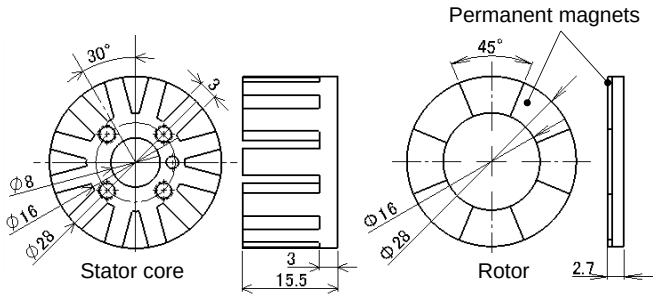

Figure 6. Geometric parameters of developed motor stator core and levitated rotor including permanent magnets

bulk soft iron (SUY-1). The permanent magnets are made of Nd-Fe-B which has a coercivity of 907 kA/m and a residual flux density of 1.36 T. The number of turns in concentrated windings wound on each stator tooth are 58. The diameter of isolated copper wire is 0.3 mm.

C. 5-DOF control system

A diagram of 5-DOF control system is shown in Fig. 7. Three eddy current sensors (PU-03A, Applied Electronics Corporation) are set onto inner side of stator tooth to measure axial position and inclination angles around x and y axes of the levitated rotor. Other two eddy current sensors are set on x-axis and y-axis to measure radial positions of the levitated rotor. Three Hall Effect sensors (Asahi KASEI Corporation) are set at stator slots to detect the rotating angles of the levitated rotor with a sensitivity of 30° electrical angle. The rotating speed is determined by calculating time derivative of rotating angles. 5-DOF control and rotating speed regulation are carried out with digital PID controllers that are implemented on a micro-processor board DS1104 (dSPACE GmbH, Paderborn Germany) with MATLAB/Simlink. Power amplifier (PA12A, Apex Microtechnology Corporation) supplies the calculated command excitation current to control windings of both stators. Sampling and control frequency is 10 kHz.

A block diagram for axial position and rotation control is shown in Fig. 8. The axial position of the levitated rotor is stabilized by regulating d-axis current i_d with a PID feedback loop. The PID controller calculate i_d from the error between detected axial position z and target axial position z^*. The target position z^* is the center of the motor, and it is set to zero. Positive and negative d-axis currents which are for field strengthening and field weakening generate an unbalanced magnetic attractive force in rotor axial direction. The rotating

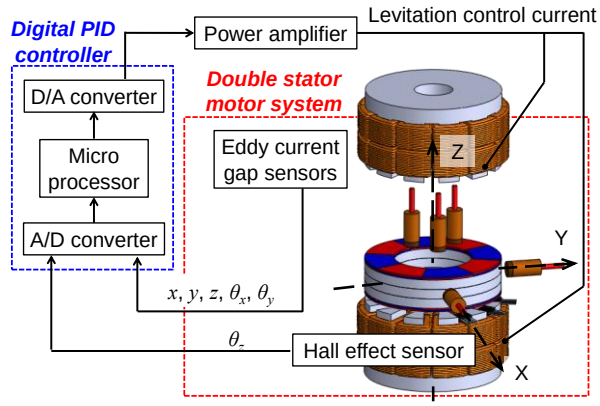

Figure 7. Feedback control system of proposed 5-DOF controlled self-bearing motor

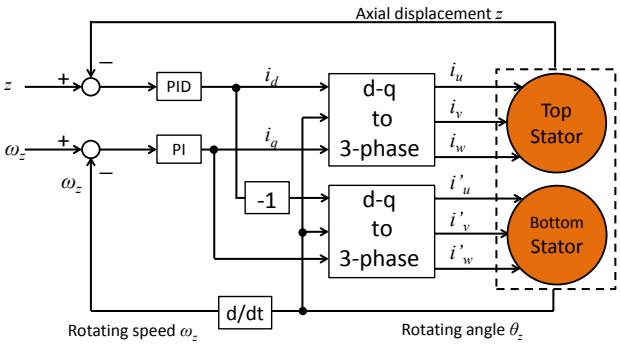

Figure 8. Block diagram for axial position and rotation control system with vector control algorithm

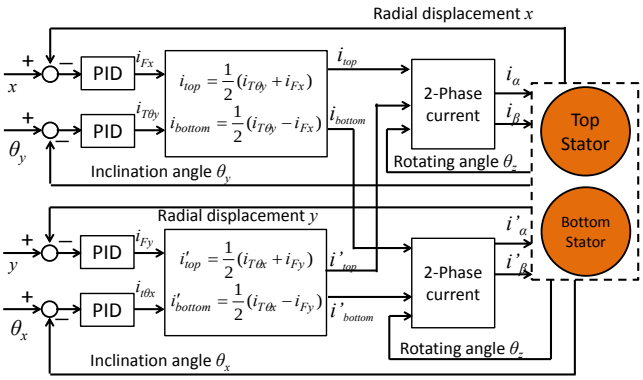

Figure 9. Block diagram for inclination and radial position control system with P±2 pole algorithm

speed is controlled by regulating q-axis current i_q with the PI feedback loop. The detected rotating speed ω_z is compared with a target rotating speed ω_z^*. The calculated q-axis current for both stator windings are equal to i_q. The d-axis current i_d and the q-axis current i_q are transformed into three-phase current i_u, i_v and i_w. Then these currents supplied to axial position and rotation control windings of both stators to generate eight pole rotating magnetic field.

A diagram for inclination angle and radial position control is shown in Fig. 9. The inclination angle θ_y control corresponds to radial position x control, and the inclination angle θ_x control corresponds to the radial position y control.

The inclination angles and the radial positions of the levitated rotor are controlled by regulating the amplitude, the direction of the restoring torque and the radial suspension force. The required excitation current for generating the restoring torque and the radial suspension force, $i_{T\theta y}$ and i_{Fx}, are calculated with PID feedback loop. The excitation current for top stator and bottom stator, i_{top} and i_{bottom}, are determined from $i_{T\theta y}$ and i_{Fx} respectively. In a similar manner, excitation current i'_{top} and i'_{bottom} that are to control inclination angle θ_x and radial position y are calculated with another PID feedback loop. The amplitude and phase angle of the two-phase current i_a, i_b, i'_a and i'_b are determined from i_{top}, i_{bottom}, i'_{top} and i'_{bottom} respectively. Consequently, these excitation currents are supplied to the inclination angle and radial position control windings to generate six poles rotating magnetic field.

D. Radial suspension force and stiffness measurement

The primary objective of the study was to determine the radial suspension capability of proposed 5-DOF controlled self-bearing motor. Initially, the radial suspension forces with varying excitation currents and radial displacements were measured. A radial force measurement system is shown in Fig. 10. The rotor is fixed to a linear slider connected with a load cell in order to restrict the rotor movement in the axial direction z and the rotational direction θ_x, θ_y. At first, both centers of the rotor and stator are aligned. The radial suspension forces were evaluated by changing the excitation current from -2 A to 2 A. The radial restoring forces were then measured by displacing the rotor radially from the center position up to 1.0 mm with micrometer at the excitation of 0 A.

E. Frequency response of radial position control

The 5-DOF controlled self-bearing motor was assembled as shown in Fig. 11, and combined with the digital control system. The rotor was levitated without rotation. The initial parameters for the PID controller were determined based on the limit sensitivity method. The optimized gains were then tuned manually as shown in Table I. The frequency response of radial position control system was measured with a frequency sweeping method using a FFT analyzer (DS-2100, DS-0264, Ono Sokki Corporation). A sinusoidal disturbance was added to the measured radial position and the disturbance frequency was varied from 1 Hz to 1 kHz.

F. Comparison of 5-DOF control and 3-DOF control

The magnetic suspension characteristics in the radial directions (x, y) were evaluated under 3-DOF control and 5-DOF control in order to demonstrate the advantages of proposed 5-DOF control. The movable range of levitated rotor in radial and axial directions was ± 0.5 mm and ± 0.3 mm, respectively. The inclination range of the levitated rotor was $\pm 1°$. The PID gains of the 5-DOF control were same as given in Table I. In case of the 3-DOF control, PID gains of the radial position controller were zero. The P gain and I gain of a rotating speed PI controller were 0.00075 A/rpm and 0.007 A/(sec・rpm). As a first step, the radial vibration waveforms at a rotating speed of 0 rpm were evaluated. Then, the levitated rotor was accelerated in rotational direction θ_z, and maximum oscillation amplitudes in the radial direction were measured. The maximum oscillation amplitude was defined as half of the peak-to-peak value of rotor vibration.

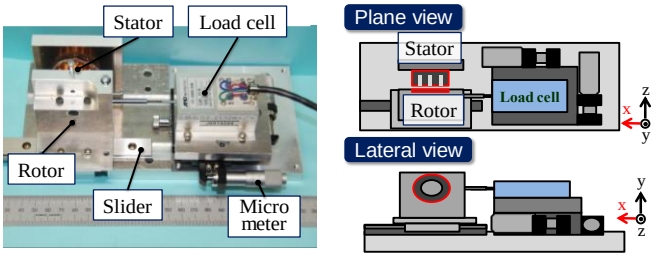

Figure 10. Experimental setup to measure the radial suspension force characteristics

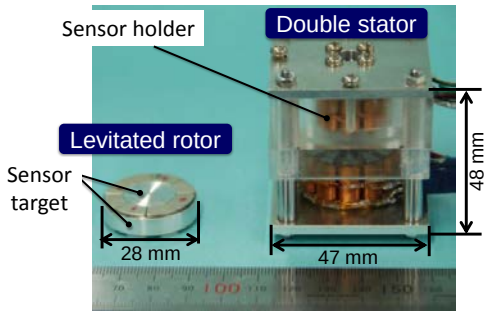

Figure 11. Photograph of assembled 5-DOF controlled self-bearing motor

TABLE I. PID CONTROLLER GAINS FOR 5-DOF CONTROLLER

Gain	Radial position	Axial position	Inclination angle
P	2.73 [A/mm]	10 [A/mm]	2.0 [A/deg]
I	0 [A/sec mm]	0.01 [A/sec mm]	0.024 [A/sec deg]
D	0.045 [A sec/mm]	0.01 [A sec/mm]	0.003 [A sec/deg]

III. EXPERIMENTAL RESULTS

A. Radial stiffness measurement

The developed motor produced radial suspension force according to proposed radial position control concept. The relationship between the radial suspension force and the excitation current is displayed in Fig. 12 (a). The developed 5-DOF controlled self-bearing motor produced radial suspension force of ± 0.8 N by varying excitation current from -2 A to 2 A. The radial suspension force to excitation current gradient of developed motor was 0.4 N/A. An acceleration coefficient defined as a mass specific force index to indicate the dynamic suspension ability was 16 m/s^{2}A. The radial restoring force with different rotor positions are shown in Fig. 12 (b). The restoring force is proportional to the radial displacement, and that gradient of the least square approximation showed a radial stiffness of 0.4 N/mm.

B. Frequency response of radial position control

Fig. 13 shows the bode diagrams of radial position control system. The results displayed similar characteristics in x direction and y direction. The resonant peaks in x and y directions are observed at 24 Hz and 30 Hz. The frequency bandwidths are 125 Hz in x direction and 112 Hz in y direction.

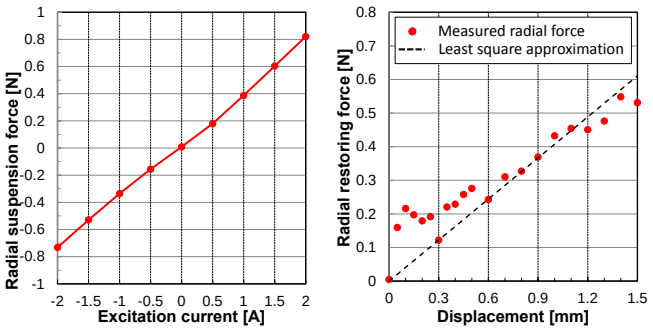

(a) (b)

Figure 12. Measured radial suspension force: (a) Force and excitation current characteristics, (b) Force and rotor radial displacement characteristics

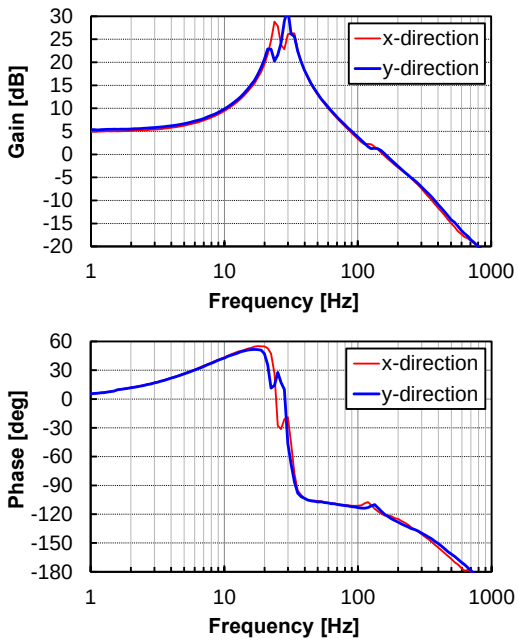

Figure 13. Bode diagrams obtaind from the results of frequency respons of radial position control system

C. *Comparison of 5-DOF control and 3-DOF control*

Fig. 14 shows the vibration waveforms of levitated rotor in radial directions at rotating speed of 0 rpm. The vibration amplitudes were less than 10 μm in both the 3-DOF control and the 5-DOF control. However, the levitated rotor was periodically fluctuated in the radial direction under the 3-DOF control as shown in Fig. 14 (a). The periodical radial fluctuation of the levitated rotor was sufficiently suppressed with 5-DOF control as shown in Fig. 14 (b).

The rotor was successfully levitated and rotated without any physical contact. The radial oscillation amplitudes of the levitated rotor with the 3-DOF control and the 5-DOF control are shown in Fig. 15. The maximum rotating speed of developed motor was expanded from 5400 rpm to 6400 rpm by implementing the 5-DOF control. Under the 3-DOF control, the double peaks of radial oscillation amplitude were observed with the rotating speeds under 2000 rpm. Except peak oscillations, the radial oscillation amplitudes were around 100 μm. By contrast, under the 5-DOF control, with rotating speeds under 2000 rpm, the resonances were

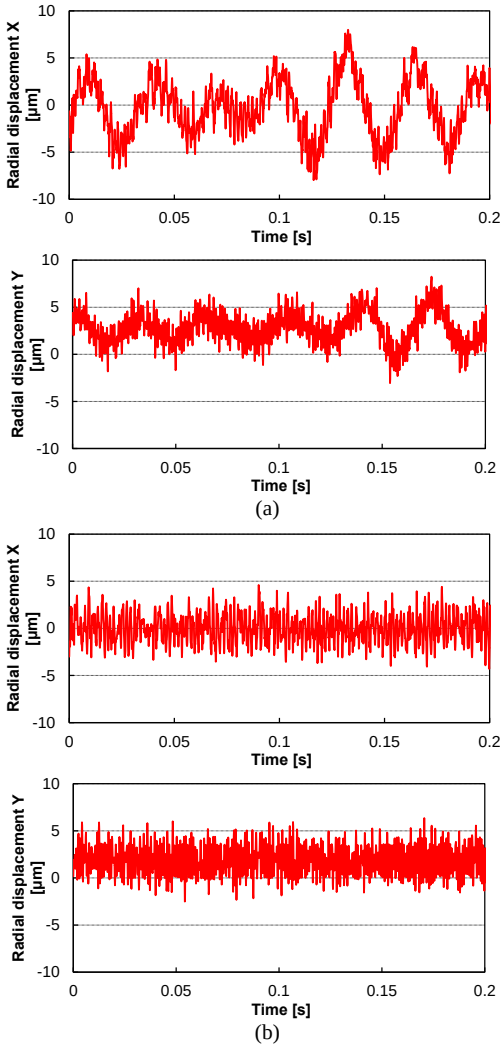

Figure 14. Radial displacement waveforms of levitated rotor at a rotating speed of 0 rpm: (a) 3-DOF of levitated rotor postures were controlled, (b) 5-DOF of levitated rotor postures were controlled

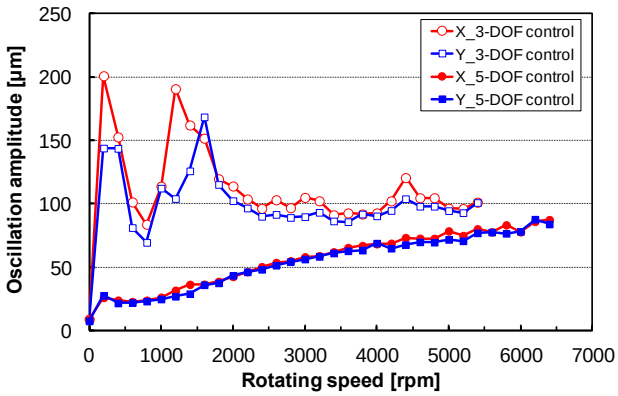

Figure 15. Maximum oscillation amplitudes in X and Y direcitions when the rotor is levitated and rotated.

successfully suppressed with the radial position active control. The oscillation amplitudes were less than 80 μm over every rotating speeds. These results demonstrate the potential of proposed radial position active control.

IV. DISCUSSION

Magnetic suspension technique is a strong candidate for VADs to improve device durability and reduce blood distraction. In the implantable paediatric VAD, size of magnetic suspension system is severely limited and magnetic air-gap is relatively large. The newly proposed 5-DOF controlled double stator axial gap self-bearing motor is one of the appropriate concepts to miniaturize the magnetically levitated system with large air-gap and guarantee non-contact stable levitation.

The results of developed radial suspension force shown in Fig.12 (a) indicate that the amplitude and direction of the radial suspension force are able to be regulated by varying excitation current. The radial position control system is further stabilized by utilizing the radial restoring force according to the rotor radial displacement. By assuming viscoelasticity of the air negligible, the radial position control system can be described as single DOF spring-mass system. A natural frequency of the system was calculated to be 28 Hz by using double stator radial stiffness of 0.8 N/mm and the levitated rotor weight of 25 g. Effects on radial fluid forces developed in the pump cavity and dumping force derived from the viscoelasticity of blood must be considered in a blood pump operation.

The frequency response tends to the vibration characteristics of the single DOF spring-mass system. The resonant frequencies in x and y directions are approximately equal to calculated natural frequency of 28 Hz. The low suppression of resonant frequency comes from weak performance of the radial suspension force production. Higher suppression performance would be achieved by optimizing the magnetic circuit geometries and combination of the pole number.

At the rotating speed of 0 rpm, the magnetically levitated rotor was fluctuated periodically under the 3-DOF control. The most dominant frequency components of the rotor fluctuation in x and y directions were analyzed with Fast Fourier transform, and these were calculated as 25 Hz in the x direction and 28 Hz in the y direction. The dominant frequencies were approximately equal to both calculated natural frequencies and the resonant frequencies observed from the bode diagrams.

The magnetic suspension performance of the developed motor was sufficient to maintain non-contact suspension and rotation at required rotating speeds for the paediatric VAD. At every rotating speed, the maximum radial oscillation amplitudes were much smaller than initial clearance of 500 μm with both the 3-DOF control and the 5-DOF control. However, under the 3-DOF control, the maximum oscillation amplitude increased at rotating speeds of 300 rpm, 1600 rpm and 1800 rpm. The first increase of radial oscillation was due to unstable characteristics at lower rotating speeds. The second increase of the radial oscillation at rotating speeds of 1600 rpm and 1800 rpm was caused by resonance when the angular frequencies come close to the resonant frequencies. By contrast, the instability at lower rotating speeds and the resonant were suppressed with the radial position control, and the proposed 5-DOF control concept demonstrated a potential of the stable levitation and rotation.

Future tasks are to develop a magnetically suspended paediatric VAD with developed 5-DOF controlled self-bearing motor and to evaluate the pump performance as well as the magnetic suspension ability and the rotor dynamics during pumping. Future design of the levitation system will focus on considering the effect of hydraulic force and viscoelastic characteristics.

V. CONCLUSIONS

The novel concept which can actively control 5-DOF of rotor postures by utilizing two types of magnetic fields based on the vector control algorithm and the P±2 pole algorithm was proposed for paediatric VAD. The proposed motor produced the sufficient radial suspension force to suspend the levitated rotor radially. The developed 5-DOF controlled self-bearing motor was successful with stable levitation and rotation. The resonances in the rotor radial directions were significantly suppressed with radial position active control. The results verified the sufficient radial position control capability and structure of 5-DOF controlled self-bearing motor.

REFERENCES

[1] J. Timothy Baldwin, Harvey S. Borovets, Brian W. Duncan, Mark J. Gartner, Robert K. Jarvik, William J. Weiss and Tracey R. Hoke, The National Heart, Lung, and Blood Institute Pediatric Circulatory Support, Journal of the American heart association, PP. 147-155, 2006.

[2] Marc Gibber, Zhongjun J. Wu, Won-Bae Chang, Giacomo Bianchi, Jingping Hu, Jose Garcia, Robert Jarvik, Bartley P. Griffith, In Vivo Experience of the Child-Size Pediatric Jarvik 2000 Heart: Update, ASAIO Journal, Vol. 56, No. 4, 2010.

[3] Noh, M.D., Antaki, J.F., Ricci, M.Gardiner, MagneticLevitation Design for the PediaFlow Ventricular Assist Device, Proc. 2005 IEEE/ASME International Conference on Advanced Intelligent Mechatronics, pp. 1077-1082, 2005.

[4] Setsuo Takatani, Hideo Hoshi, Kennichi Tajima, Katsuhiro Ohuchi, Makoto Nakamura, Tadahiko Shinshi, Masaharu Yoshikawa, Feasibility of a Miniature Centrifugal Rotary Blood Pump for Low-Flow Circulation in Children and Infants, ASAIO Journal, Vol. 51, No. 5, pp. 557-562, 2005.

[5] Daniel L. Timms, Nobuyuki Kurita, Nicholas Greatrex, Toru Masuzawa, BiVACOR A Magnetically Levitated Biventricualr Artificial Heart, Proc. of MAGDA conference in Pacific Asia, pp.482-487, 2011.

[6] Hideo Hoshi, Tadahiko Shinshi, Setsuo Takatani, Third-generation Blood Pumps With Mechanical Noncontact Magnetic Bearings, Artificial Organs, Vol. 30, No. 5, pp. 324-338, 2006.

[7] David J. Farrar, Kevin Bourque, Charles P. Dague, Christopher J. Cotter, Victor L. Poirier, Design Features, Developmental Status, and Experimental Results With the Heartmate III Centrifugal Left Ventricular Assist System with a Magnetically Levitated Rotor, ASAIO Journal, Vol. 53, No. 3, pp. 310-315, 2007.

[8] Atsushi Yumoto, Tadahiko Shinshi, Xiayou Zhang, Hiroyuki Tachikawa, Akira Shimokohbe, A One-DOF Controlled Magnetic Bearing for Compact Centrifugal Blood Pumps, Motion and Vibration Control, Springer Science+Business Media B.V. , pp. 357-366, 2009.

[9] Masahiro Osa, Toru Masuzawa, Eisuke Tatsumi, Miniaturized axial gap maglev motor with vector control for pediatric artificial heart, Journal of JSAEM, Vol. 20, No. 2, pp. 397-403, 2012.

[10] Junichi Asama, Yuki Hamasaki, Takaaki Oiwa, Akira Chiba, Proposal and Analysis of a Novel Single-Drive Bearingless Motor, IEEE Transactions on Industrial Electronics, Vol. 60, No. 1, pp. 129-138, 2013.

[11] Quang Dich Nguyen, Satoshi Ueno, Analysis and Control of Nonsalient Permanent Magnet Axial Gap Self-Bearing Motor, IEEE Transactions on Industrial Electronics, Vol. 58, No. 7, pp. 2644-2652, 2011.

[12] Satoshi Ueno, Yoji Okada, Characteristics and Control of a Bidirectional Axial Gap Combined Motor-Bearing, IEEE/ASME Transactions on Mechatronics, Vol. 5, No. 3, pp. 310-318, 2000.

[13] Masahiro Osa, Toru Masuzawa, Eisuke Tatsumi, 5-DOF control double stator motor for paediatric ventricular assist device, Proceedings of ISMB13, paper41, 2012